



ELSEVIER

Contents lists available at ScienceDirect

## Bioorganic &amp; Medicinal Chemistry Letters

journal homepage: [www.elsevier.com/locate/bmcl](http://www.elsevier.com/locate/bmcl)

## PB-10, a thiazolo[4,5-d] pyrimidine derivative, targets p21-activated kinase 4 in human colorectal cancer cells

Ruijuan Li<sup>a,b</sup>, Hanxun Wang<sup>b</sup>, Jian Wang<sup>b,\*</sup>, Maosheng Cheng<sup>b,\*</sup>

<sup>a</sup> College of Pharmacy, Inner Mongolia Medical University, Huhhot 010110, PR China

<sup>b</sup> Key Laboratory of Structure-Based Drug Design & Discovery of Ministry of Education, School of Pharmaceutical Engineering, Shenyang Pharmaceutical University, Shenyang 110016, PR China

## ARTICLE INFO

## Keywords:

p21-Activated kinase 4  
Inhibitor  
Thiazolo[4,5-d]pyrimidine  
Colorectal cancer

## ABSTRACT

Targeting p21-activated kinase 4 (PAK4) is a potential therapeutic strategy against human colorectal cancer (CRC). In this study, we synthesized a series of novel thiazolo[4,5-d]pyrimidine derivatives (PB-1–12) and identified PB-10 (PAK4 IC<sub>50</sub> = 15.12 μM) as a potential and potent PAK4 inhibitor. Our results showed that PB-10 significantly suppressed the proliferation and colony formation of human CRC cells. PB-10 also arrested HCT-116 CRC cells at sub G0/G1 phase while promoting the expression of proapoptotic proteins. In addition, PB-10 inhibited migration, invasion, and adhesion as well as the PAK4 downstream signaling pathway in HCT-116 cells. Molecular docking analysis showed possible binding modes between PB-10 and PAK4. Our study provides a novel compound that may block the PAK4 signaling in CRC cells.

p21-Activated kinase 4 (PAK4) belongs to the PAK family of serine/threonine kinases, playing important roles in tumorigenesis and progression in human cancers by regulating anchorage-independent growth, cell cycle, survival, migration, and invasion in cancer cells.<sup>1–4</sup> PAK4 overexpression has been detected in multiple cancer types, including colorectal cancer (CRC).<sup>5</sup> Elevated expression of PAK4 correlates with advanced tumor stage and poor prognosis in CRC patients; and PAK4 silencing can inhibit CRC cell proliferation while inducing cell cycle arrest and apoptosis.<sup>4–6</sup> Therefore, targeting PAK4 is a promising therapeutic strategy against CRC.

As a p21-activated protein kinase that phosphorylates multiple downstream genes, PAK4 is activated by p21 proteins via phosphorylation on its activation loop, which triggers conformational movements in its catalytic cleft to exchange nucleotide.<sup>7,8</sup> Scientists have developed various ATP-competitive compounds, such as Staurosporine, LCH-7749944, PF-3758309, and KPT-9274, to inhibit phosphorylation or conformational movements of PAK4.<sup>9–12</sup> Although these compounds are pan-PAK inhibitors due to the highly-conserved ATP-binding pocket across the PAK family and did not progress beyond phase I clinical trials, they provide helpful rationale and scaffolds for the development of more selective and potent PAK4 inhibitors as anticancer therapeutics.<sup>13,14</sup>

Thiazolo[4,5-d]pyrimidines and their derivatives are purine analogues that display diverse pharmacological properties, including antitumor, antimicrobial, and antiinflammatory activities.<sup>15–17</sup> In our

previous studies, using a structure-based virtual screening strategy, we identified a thiazolo[4,5-d]pyrimidine-derived compound ZINC28569592 as a promising hit compound toward PAK4 with a half-maximal inhibitory concentration (IC<sub>50</sub>) of 18.42 μM.<sup>18,19</sup> In this study, starting from the structure of ZINC28569592, we synthesized a series of novel thiazolo[4,5-d]pyrimidine derivatives (PB-1–12) with various structural modification (Fig. 1). In this new series, the chlorine atom at C7-position of thiazolo[4,5-d]pyrimidine ring was replaced by an amine portion, substituted by alkylic, cycloalkylic, arylalkylic residues. The replacement of the chlorine by the amine function was not expected to affect the potency of these compounds to bind the PAK4 active binding site, and to establish hydrophobic-bond interactions with the amino acid residues in the hydrophobic entrance of PAK4 active site. We evaluated the inhibitory activity of these novel synthesized compounds PB-1–12 toward PAK4, and PB-10 was identified as a novel and potent lead compound targeting PAK4 in human CRC cells, providing a new therapeutic approach against CRC.

Synthesis of the designed thiazolo[4,5-d]pyrimidine derivatives PB-1–12 employed 5-(benzylthio)-7-chlorothiazolo[4,5-d]pyrimidin-2-amine (6) as the key intermediate.<sup>20</sup> This intermediate was obtained from thiocarbamide (1) through the synthetic methodology. Treatment of 1 with ethyl cyanoacetate and sodium ethoxide at 78 °C provided a good yield of 2. Then, the resulting intermediate 2 was subjected to nucleophilic substitution with benzyl bromide to produce 3. The C4-position hydrogen of 3 was selectively substituted with bromine, and

\* Corresponding authors.

E-mail addresses: [jianwang@syphu.edu.cn](mailto:jianwang@syphu.edu.cn) (J. Wang), [mscheng@syphu.edu.cn](mailto:mscheng@syphu.edu.cn) (M. Cheng).

<https://doi.org/10.1016/j.bmcl.2019.126807>

Received 13 July 2019; Received in revised form 8 October 2019; Accepted 4 November 2019

0960-894X/ © 2019 Elsevier Ltd. All rights reserved.

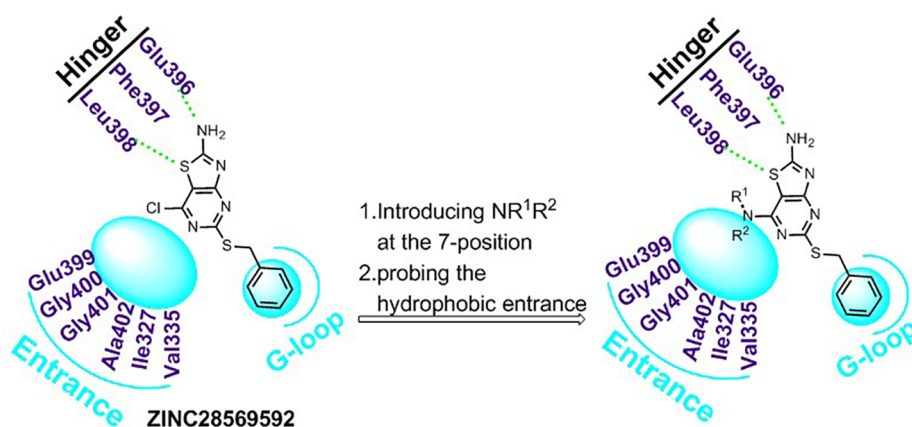
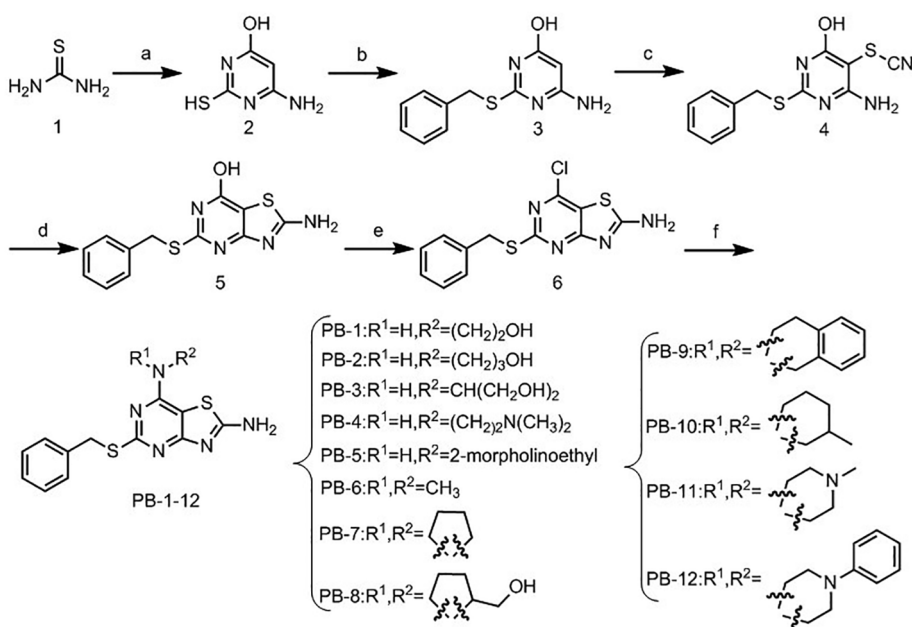


Fig. 1. Design of novel thiazolo[4,5-*d*]pyrimidine derivatives starting from the hit compound ZINC28569592.



then was subjected to nucleophilic substitution with potassium thiocyanate to give 4. This intermediate 4 was treated with cyclization at 110 °C provided 5. Then, the resulting intermediate 5 was subjected to chlorination with phosphoryl trichloride to give the key intermediate 6. Finally, the chlorine at the C7-position of 6 was substituted with available aliphatic amine and cyclamine derivatives in the presence of 1-methyl-2-pyrrolidinone to provide the target compounds PB-1–12 (Scheme 1). These compounds were purified by column chromatography or crystallization, and then were submitted to biological evaluation.

The activity of the target compounds PB-1–12 toward PAK4 was investigated by homogeneous time resolved fluorescence (HTRF) assay. The classical pan-PAK inhibitor staurosporine and the hit compound ZINC28569592 were used as reference compounds. In the preliminary screening assay, all derivatives inhibited PAK4 activity in a dose-dependent manner (Fig. 2). Seven compounds (PB-1, 4, 6, 8, 10, 11, and

12) that demonstrated moderately inhibited PAK4 with percentages of inhibition more than 50% were further tested over a broader concentration range. As shown in Table 1, only compound PB-10 was slightly more potent than hit compound ZINC28569592. However, we found that with flexible carbon chain extension of alkylic amine at C7-position of thiazolo[4,5-*d*]pyrimidine ring, compounds PB-6, PB-1, PB-4 and PB-5 presented a decrease in inhibition toward PAK4. Meanwhile, in order to investigate the effect of reducing the flexibility and increasing the lipophilic space volume of the alkylic amine function on compounds activity, compounds PB-1 (42.13 μM), PB-4 (89.5 μM) and PB-6 (32.03 μM) were cyclized to obtain cyclic amines compounds PB-8 (34.1 μM), PB-11 (70.63 μM) and PB-10 (15.12 μM), respectively. Interestingly, replacement of flexible alkylic amine group with the cyclic aliphatic amine group led to a slightly increase in the activity. These data obtained suggest that the steric hydrophobic group on the aliphatic amine moiety are important, but not crucial in producing an effective

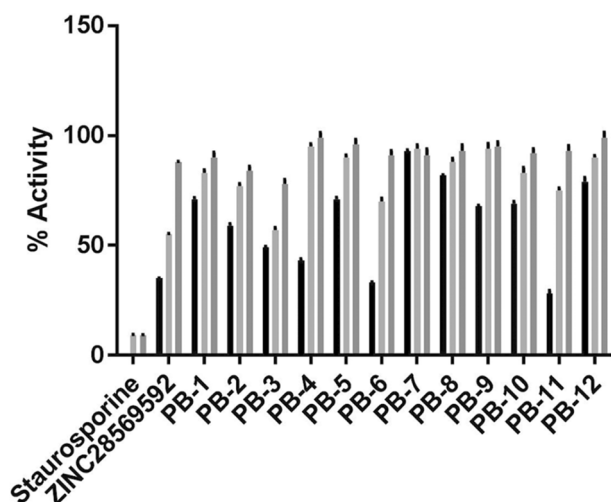


**Fig. 2.** Homogenous time-resolved fluorescence (HTRF) assay of p21-activated kinase 4 (PAK4) activity. The 20 mM DMSO stock solution of each compound (PB-1–12) was serially diluted in kinase reaction buffer at 100, 10, and 1  $\mu$ M, respectively. The PAK4 activity was determined using HTRF assay. The pan-kinase inhibitor staurosporine and compound ZINC28569592 were used as positive controls. Data are expressed as mean  $\pm$  standard deviation (SD). n = 3.

**Table 1**

The inhibitory activities of thiazolo[4,5-d]pyrimidine derivatives against PAK4. N/A, Not applicable.

Compounds	RN	IC <sub>50</sub> <sup>a</sup> ( $\mu$ M)
PB-1	NH(CH <sub>2</sub> ) <sub>2</sub> OH	42.13
PB-2	NH(CH <sub>2</sub> ) <sub>3</sub> OH	NT <sup>b</sup>
PB-3	NHCH(CH <sub>2</sub> OH) <sub>2</sub>	NT <sup>b</sup>
PB-4	NH(CH <sub>2</sub> ) <sub>2</sub> N(CH <sub>3</sub> ) <sub>2</sub>	89.5
PB-5	2-morpholinoethan-1-amino	> 100
PB-6	N,N-dimethylamino	32.03
PB-7	Pyrrolidin-1-yl	NT <sup>b</sup>
PB-8	2-hydroxymethylpyrrolidin-1-yl	34.1
PB-9	3,4-dihydroisoquinolin-2(1H)-yl	NT <sup>b</sup>
PB-10	3-methylpiperidin-1-yl	15.12
PB-11	4-methylpiperazin-1-yl	70.63
PB-12	4-phenylpiperazin-1-yl	44.11
ZINC28569592 <sup>c</sup>		18.42
Staurosporine <sup>c</sup>		0.001

<sup>a</sup> IC<sub>50</sub> values are calculated based on the homogeneous time-resolved fluorescence (HTRF) assay.

<sup>b</sup> NT: not tested in this assay.

<sup>c</sup> Used as a positive control.

**Table 2**

The antiproliferative effect of PB-10 on different colon cancer cell lines.

Compounds	IC <sub>50</sub> <sup>a</sup> ( $\mu$ M)		
	HCT116	SW480	Colo205
PB-10	4.3172	6.5962	7.8047
Staurosporine	< 0.1	< 0.1	< 0.1

<sup>a</sup> IC<sub>50</sub>: concentration of the compound ( $\mu$ M) producing 50% cell growth inhibition after 48 h of drug exposure, as determined by the MTT assay. Each experiment was carried out in triplicate.

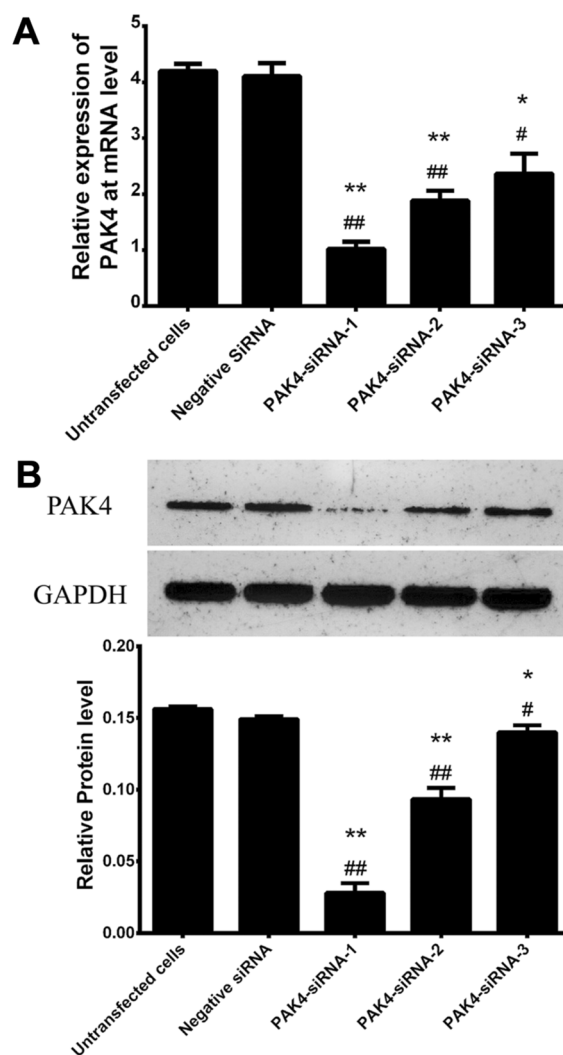


**Fig. 3.** Small interfering RNA (siRNA)-mediated PAK4 silencing. HCT-116 cells were cultured overnight and then transfected with GFP-labelled negative control, siRNA-1, siRNA-2, or siRNA-3 against PAK4 using Lipofectamine 2000. At 48 h after transfection, the mRNA (A) and protein (B) levels of PAK4 were determined using quantitative real-time PCR (qRT-PCR) and Western blot analysis, respectively. GAPDH was used as an internal control. Data are expressed as the mean  $\pm$  standard deviation (SD). \**P* < 0.05, \*\**P* < 0.01 vs untransfected cells; #*P* < 0.05, ##*P* < 0.01 vs Negative-siRNA transfected cells. n = 3.

inhibition toward PAK4. This finding may provide directions for further structural modifications for designing potent PAK4 inhibitors. Among these novel compounds, the most potent inhibitor PB-10 was selected for further exploration.

To investigate the potential antitumor activity of PB-10, we explored the effects of PB-10 on the proliferation of different human CRC cell lines *in vitro*. As shown in Table 2, PB-10 inhibited the cell viability of HCT-116, SW480, and Colo205 cells with IC<sub>50</sub> values of 4.3, 6.5, and 7.8  $\mu$ M, respectively. HCT-116 cells with the lowest IC<sub>50</sub> were used in the following study.

We then compared the effects of PB-10 (4.3  $\mu$ M) treatment and knockdown of PAK4 on HCT-116 cell proliferation and colony

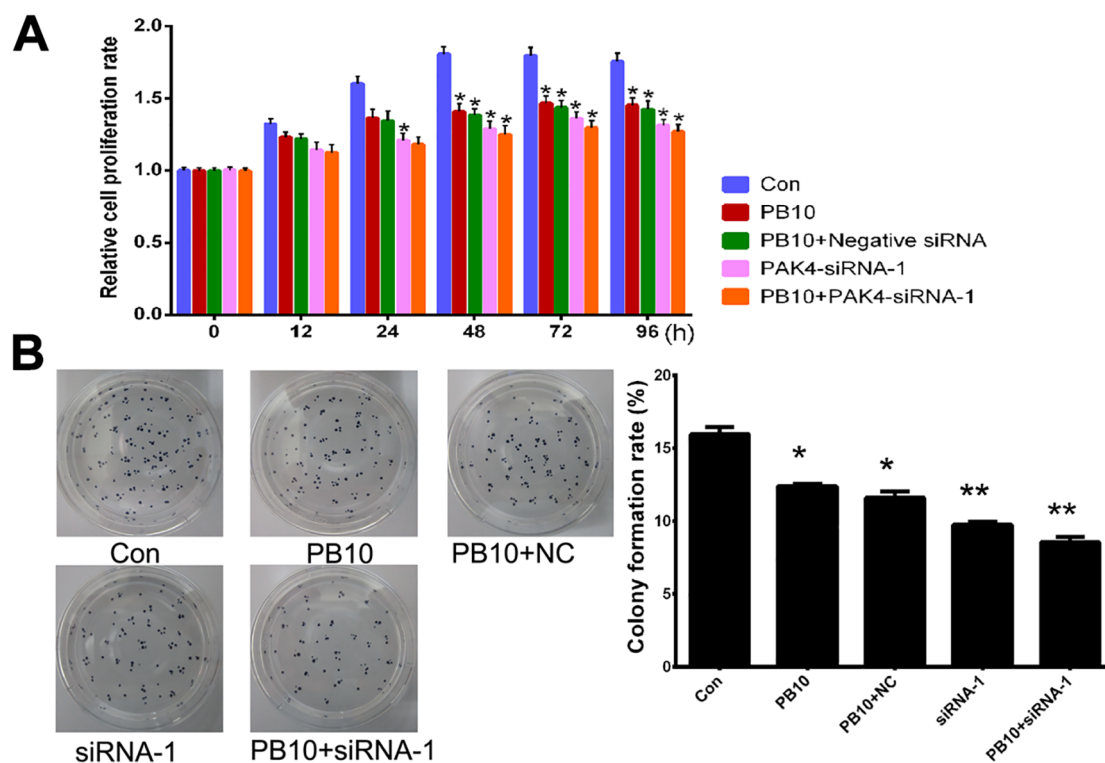


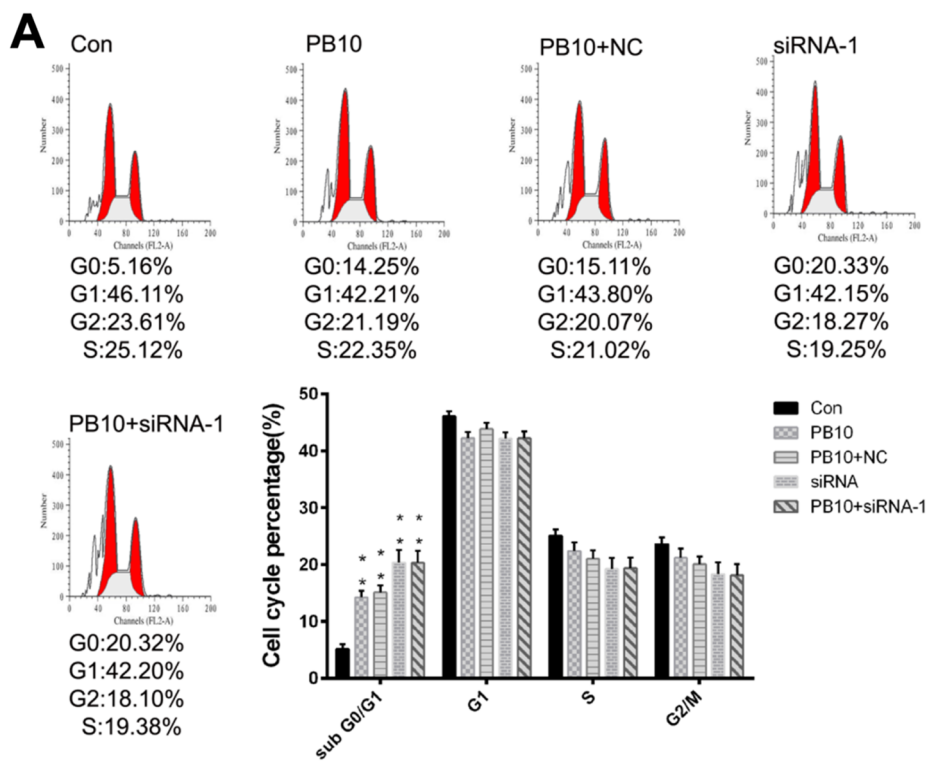
**Fig. 4.** Cell proliferation and colony formation assays. HCT-116 cells were treated with PB-10 (4.3  $\mu$ M) and/or transfected with PAK4-siRNA1. (A) MTT cell viability assay was performed at different time points (0, 12, 24, 48, 72, and 96 h) after treatment/transfection. (B) Colony formation was assessed at 2 weeks after treatment/transfection. Cells were stained with crystal violet. Images were acquired using SONY camera. Representative images are shown. The colony formation rate (%) was calculated as Clonal formation rate = (number of clones / number of cells inoculated)  $\times$  100%. Data are expressed as the mean  $\pm$  SD. \* $P$  < 0.05, \*\* $P$  < 0.01 vs control group.  $n$  = 3. (For interpretation of the references to color in this figure legend, the reader is referred to the web version of this article.)

formation. The siRNA knockdown efficiency was shown in Fig. 3. As shown in Fig. 4A and B, PB-10 or PAK4 silencing could observably inhibit HCT-116 cell proliferation and colony formation. To further investigate whether the inhibitory effect of PB-10 on cell proliferation was due to the induction of cell cycle arrest and apoptosis, we examined the cell cycle and apoptosis-related protein levels in PB-10-treated HCT-116 cells. As shown in Fig. 5A, PB-10 or PAK4 silencing significantly increased the percentage of cells in the G0/G1 phase compared with vehicle treatment. In addition, Western blot assay showed that PB-10 markedly attenuated the expression of PAK4 while inducing the expression of proapoptotic caspase-3, BAD, and cytochrome C (Fig. 5B). PAK4 is involved in cell cycle arrest by altering the expression of various proteins such as p21 and cyclins.<sup>21–24</sup> PAK4 phosphorylates BAD and caspases, thereby promoting cell survival and preventing apoptosis.<sup>25</sup> Above studies approve that similar to the effects of PAK4 silencing, PB-10 could significantly inhibit the proliferation and colony formation while inducing cell cycle arrest and proapoptotic protein expression in HCT-116 cells.

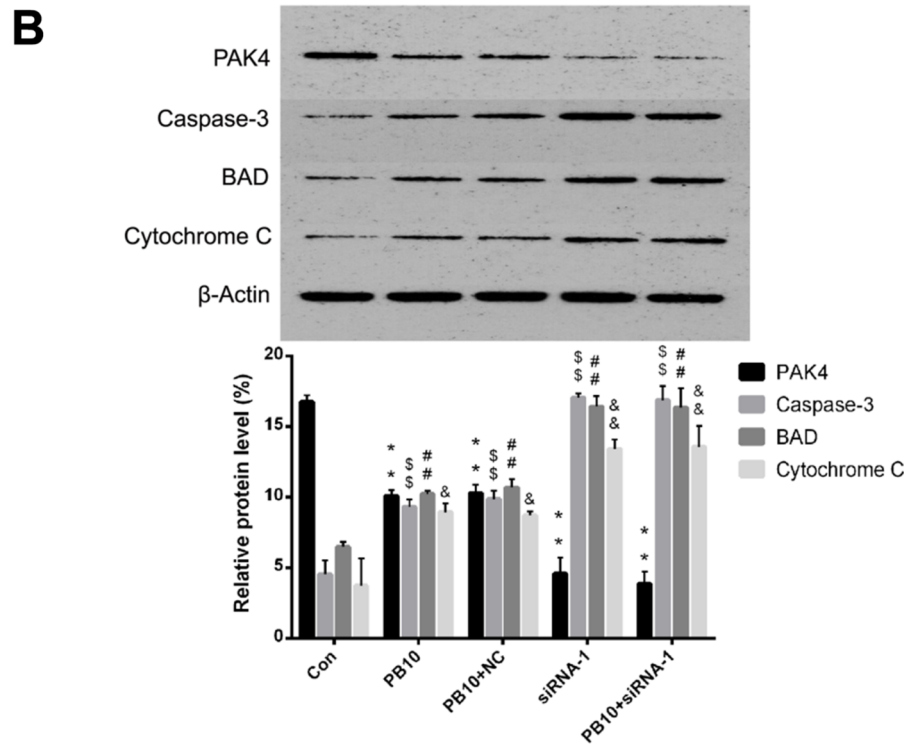
Next, we assessed the effect of PB-10 on CRC cell mobility. PB-10 or PAK4 silencing significantly suppressed HCT-116 cell migration and invasion compared with vehicle treatment (Fig. 6A and B). To regulate cell mobility, PAK4-mediated activation of cytoskeletal effector LIMK1 phosphorylates and inhibits the actin-regulatory protein cofilin.<sup>26</sup> Because the LIM kinase-1 (LIMK1)/cofilin axis is involved in PAK4-

mediated CRC cell migration and invasion, we detected the protein levels of LIMK1 and cofilin.<sup>27</sup> As shown in Fig. 6C, PB-10 or PAK4 silencing remarkably decreased the proteins levels of LIMK1 and cofilin in HCT-116 cells, suggesting that PB-10 targets PAK4 to suppress CRC cells mobility possibly through the suppression of the PAK4/LIMK1/cofilin signaling pathway. In addition, PB-10 treatment or knockdown of PAK4 also inhibited HCT-116 adhesion *in vitro* (Fig. 6D). Taken together, these results suggest that PB-10 may repress CRC progression possibly through inhibition of PAK4.

In order to gain insight into potential binding mode between PB-10 and PAK4, we performed a molecular docking analysis (Fig. 7). PB-10 could potentially bind to the hydrophobic catalytic domain of PAK4 (PDB Code: 2X4Z) via interactions with the key residues. Specifically, the sulfur atom at S1-position and the amino group at the C2-position of PB-10 can form two hydrogen binding interactions with the hinge residues Leu398 and Glu396 of PAK4; the benzylthio fragment at the C5-position of PB-10 can extend to the G-loop pocket and form hydrophobic interactions with PAK4; the thiazolo[4,5-*d*]pyrimidine ring can form a hydrophobic interactions with Ala348, Met395, Val335 or Leu447. Comparing with the hit compound ZINC28569592, the 3-methylpiperidin-1-yl at C7-position of thiazolo[4,5-*d*]pyrimidine moiety of PB-10 could occupy the inlet of the catalytic cleft via forming hydrophobic interactions with ILE327 and GLY401. The thiazolo[4,5-*d*]pyrimidine scaffold is responsible for its interactions with the ATP-binding



**Fig. 5.** Cell cycle and apoptosis analyses. HCT-116 cells were treated with PB-10 (4.3  $\mu$ M) and/or transfected with PAK4-siRNA1. (A) Cell cycle analysis was performed at 48 h after treatment/transfection using flow cytometry. The percentage of cells at different cell cycle was calculated as the cell number at each cell cycle / the total cell number  $\times$  100%. Data are expressed as the mean  $\pm$  SD. \* $P$  < 0.05 vs. control group. n = 3. (B) Western blot assay was performed at 48 h after treatment/transfection to determine the protein levels of apoptosis-related caspase-3, BAD, and cytochrome C.  $\beta$ -actin was used as an internal control. Data are expressed as the mean  $\pm$  SD. \*\* $P$  < 0.01 vs PAK4 in control group;  $^{\$}$  $P$  < 0.01 vs caspase-3 in control group;  $^{\#\#}$  $P$  < 0.01 vs BAD in control group;  $^{\&}$  $P$  < 0.05,  $^{\&\&}$  $P$  < 0.01 vs cytochrome C in control group. n = 3.



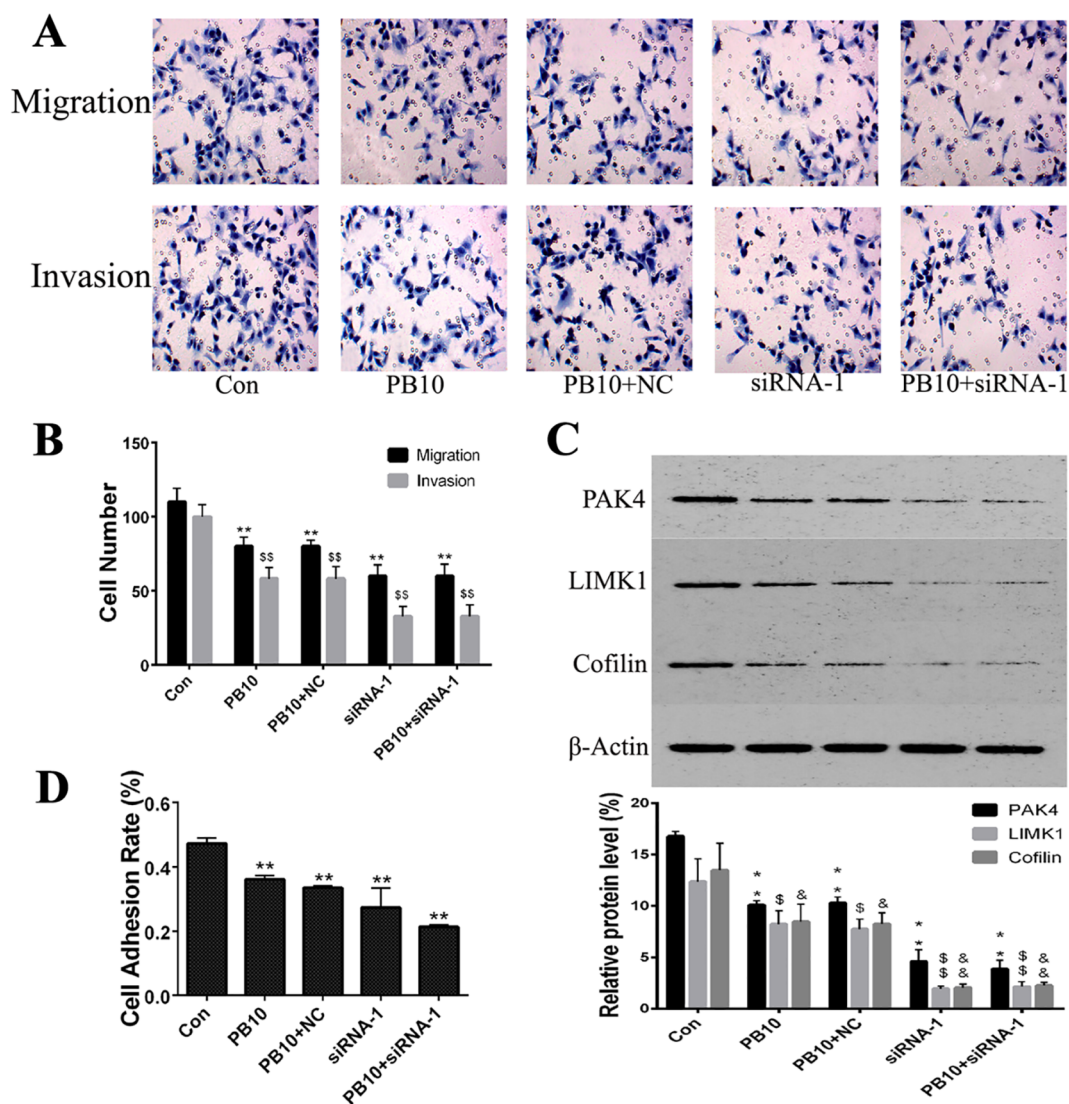


**Fig. 6.** Cell migration, invasion, and adhesion analyses. HCT-116 cells were treated with PB-10 (4.3  $\mu\text{M}$ ) and/or transfected with PAK4-siRNA1. Transwell assay was performed to evaluate cell migration and invasion at 48 h post treatment/transfection. The migrated and invaded cells were stained with crystal violet. Images were acquired at magnification  $\times 200$ . Representative images are shown in (A). (B) The numbers of migrated or invaded cells were counted in 5 randomly selected fields. Data are expressed as the mean  $\pm$  SD. \*\* $P < 0.01$  vs migrated cells in control group; <sup>ss</sup> $P < 0.01$  vs invaded cells in control group.  $n = 5$ . (C) Western blot analysis was performed at 48 h after treatment/transfection to determine the protein levels of PAK4 and downstream LIM domain kinase 1 (LIMK1) and cofilin.  $\beta$ -actin was used as an internal control. Data are expressed as the mean  $\pm$  SD. \*\* $P < 0.01$  vs PAK4 in control group;  $^*P < 0.05$ , <sup>ss</sup> $P < 0.01$  vs LIMK1 in control group;  $^*P < 0.05$ , <sup>ss</sup> $P < 0.01$  vs cofilin in control group.  $n = 3$ . (D) Cell adhesion assay was performed in fibronectin-coated plates. Cells were allowed to adhere for 2 h. The adherent cells were stained with crystal violet. The cell adhesion rate (%) was calculated as the number of adherent cells / the number of control cells  $\times 100\%$ . Data are expressed as the mean  $\pm$  SD. \*\* $P < 0.01$  vs control group.  $n = 3$ . (For interpretation of the references to color in this figure legend, the reader is referred to the web version of this article.)

region in PAK4 via hydrogen bonds. The predicted binding mode of PB-10 in PAK4 active site support that the thiazolo[4,5-*d*]pyrimidine analogue PB-10 could be as a novel lead compound for further designing more potential PAK4 inhibitors as anticancer agents.

In conclusion, starting from a hit compound 5-(benzylthio)-7-chlorothiazolo[4,5-*d*]pyrimidin-2-amine, we designed and synthesized a series of thiazolo[4,5-*d*]pyrimidine derivatives as novel and potential PAK4 inhibitors for further development as cancer therapeutics. PB-10 was identified as a potent inhibitor of PAK4 ( $\text{IC}_{50} = 15.12 \mu\text{M}$ ) and could effectively inhibit cell growth, cell mobility, and PAK4 downstream signaling pathway in HCT-116 CRC cell line while inducing cell

cycle arrest and the expression of proapoptotic proteins. Molecular docking analysis predicted the possible binding mode of PB-10 and PAK4. Above studies supported that PB-10-mediated inhibition of PAK4 is a potential therapeutic strategy against CRC.

#### Declaration of Competing Interest

The authors declare that they have no known competing financial interests or personal relationships that could have appeared to influence the work reported in this paper.

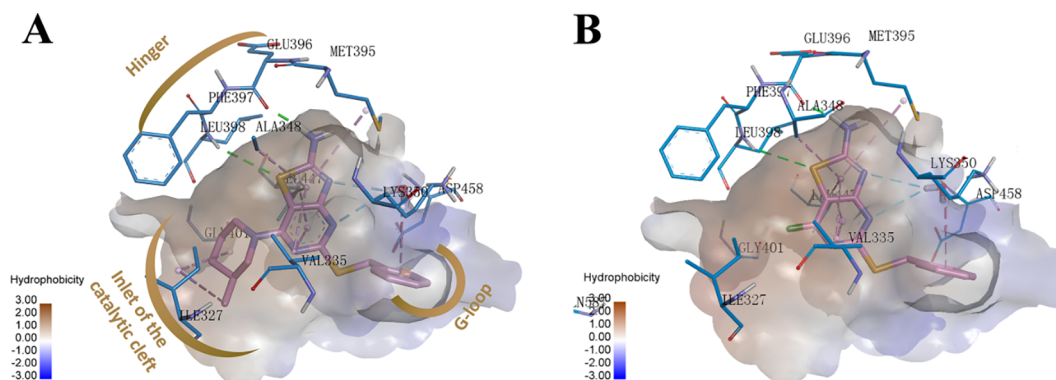


**Fig. 7.** Binding pattern of compounds and PAK4. Binding modes of lead compound PB-10 and hit compound ZINC28569592 in PAK4 active site are shown in (A) and (B), respectively. PAK4 active site is shown as a surface that is color-coded based on hydrophobicity. The characteristic partial Hinger, G-loop, and inlet of the catalytic cleft are shown as secondary structures. The classical H-bonds are shown via green dotted lines, the non-classic H-bonds are shown via pale-cyan dotted lines, and hydrophobic interactions are shown via pink dotted lines. The key amino-acid residues, PB-10 and ZINC28569592 are shown in sticks. (For interpretation of the references to color in this figure legend, the reader is referred to the web version of this article.)

## Acknowledgements

The authors gratefully acknowledge financial support from the National Natural Science Foundation of China (Grant No. 81230077, 81660587), the Natural Science Foundation of Inner Mongolia Autonomous region (Grant No. 2016BS0807), the National Natural Science Foundation of Liaoning province (Grant No. 20170540854).

## Appendix A. Supplementary data

Supplementary data to this article can be found online at <https://doi.org/10.1016/j.bmcl.2019.126807>.

## References

- Guo Q, Su N, Zhang J, et al. *Oncogene*. 2014;33:3277.
- King H, Thillai K, Whale A, et al. *Sci Rep*. 2017;7:42575.
- Kobayashi K, Inokuchi M, Takagi Y, et al. *J Clin Pathol*. 2016;69:580.
- Zhang X, Zhang X, Li Y, et al. *Cell Death Dis*. 2017;8:e2820.
- Song B, Wang W, Zheng Y, et al. *J Surg Res*. 2015;196:130.
- Tabusa H, Brooks T, Massey AJ. *Mol Cancer Res*. 2013;11:109.
- Zhang EY, Ha BH, Boggan TJ. *Biochim Biophys Acta Proteins Proteom*. 2018;1866:356.
- Ha BH, Morse EM, Turk BE, et al. *J Biol Chem*. 2015;290:12975.
- Rudolph J, Crawford JJ, Hoeflich KP, et al. *Enzymes*. 2013;34:157.
- Murray BW, Guo C, Piraino J, et al. *Proc Natl Acad Sci U S A*. 2010;107:9446.
- Zhang J, Wang J, Guo Q, et al. *Cancer Lett*. 2012;317:24.
- Abu AO, Chen CH, Senapedis W, et al. *Mol Cancer Ther*. 2016;15:2119.
- Staben ST, Feng JA, Lyle K, et al. *J Med Chem*. 2014;57:1033.
- Rudolph J, Crawford JJ, Hoeflich KP, et al. *J Med Chem*. 2015;58:111.
- Yu Z, Paul R, Bhattacharya C, et al. *Biochemistry*. 2015;54:3100.
- Kuppast B, Spyridaki K, Lynch C, et al. *Med Chem*. 2014;11:50.
- Singh B, Guru SK, Kour S, et al. *Eur J Med Chem*. 2013;70:864.
- Li RJ, Wang J, Xu Z, et al. *ChemMedChem*. 2014;9:1012.
- Li RJ, Su XL, Chen Z, et al. *RSC Adv*. 2015;5:23202.
- Sofia K, Gunnar N, Sohn D, et al. *J Med Chem*. 2013;56:3177.
- Lin R, Johnson SG, Connolly PJ, et al. *Bioorg Med Chem Lett*. 2009;19:2333.
- Nekrasova T, Minden A. *J Cell Biochem*. 2011;112:1795.
- Tyagi N, Bhardwaj A, Singh AP, et al. *Oncotarget*. 2014;5:8778.
- Li Y, Wang D, Zhang H, et al. *Anat Rec (Hoboken)* 2013;296:1561.
- Shao YG, Ning K, Li F. *World J Gastroenterol*. 2016;22:1224.
- Ye DZ, Field J. *Cell Logist*. 2012;2:105.
- Sheng N, Tan G, You W, et al. *Cancer Med*. 2017;6:1331.